Biochemical Pharmacology 83 (2012) 644–652

Contents lists available at SciVerse ScienceDirect

Biochemical Pharmacology

journal homepage: www.elsevier.com/locate/biochempharm

A truncated analogue of CCL2 mediates anti-fibrotic effects on murine fibroblasts independently of CCR2

Christina Kalderén [a,b], Margareta Forsgren [a], Ulla Karlström [a], Karin Stefansson [a], Robert Svensson [a], Magnus M. Berglund [a], Gunnar Palm [a], Martin Selander [a], Maj Sundbom [a], Joakim Nilsson [a], Annelie Sjögren [a], Kristina Zachrisson [a], Stefan Svensson Gelius [a,*]

[a] Swedish Orphan Biovitrum AB, Stockholm, Sweden
[b] Department of Medical Biochemistry and Biophysics, Karolinska Institutet, Stockholm, Sweden

ARTICLE INFO

Article history:
Received 13 October 2011
Accepted 1 December 2011
Available online 9 December 2011

Keywords:
7ND
CCL2
CCR2
Chemokine
Fibrosis

ABSTRACT

The truncated [1 + 9–76] CCL2 analogue, also known as 7ND, has been described in numerous reports as an anti-inflammatory and anti-fibrotic agent in a wide spectrum of animal models, e.g. models of cardiovascular disease, graft versus host disease and bleomycin-induced pulmonary fibrosis. 7ND has been reported to function as a competitive inhibitor of CCL2 signaling via CCR2 in human in vitro systems. In contrast, the mechanistic basis of 7ND action in animal models has not been previously reported. Here we have studied how 7ND interacts with CCL2 and CCR2 of murine origin. Surprisingly, 7ND was shown to be a weak inhibitor of murine CCL2/CCR2 signaling and displaced murine CCL2 (JE) from the receptor with a $K_i > 1$ μM. Using surface plasmon resonance, we found that 7ND binds murine CCL2 with a K_d of 670 nM, which may indicate that 7ND inhibits murine CCL2/CCR2 signaling by a dominant negative mechanism rather than by competitive binding to the CCR2 receptor. In addition we observed that sub-nanomolar levels of 7ND mediate anti-fibrotic effects in CCR2 negative fibroblasts cultured from fibrotic lung of bleomycin-induced mice. Basal levels of extracellular matrix proteins were reduced (collagen type 1 and fibronectin) as well as expression levels of α-smooth muscle actin and CCL2. Our conclusion from these data is that the previously reported effects of 7ND in murine disease models most probably are mediated via mechanisms independent of CCR2.

1. Introduction

Chemokines are a defined group of structurally related small cytokines controlling the migration of cells through signaling via specific G protein-coupled receptors (GPCRs) [1]. The chemokine CCL2/MCP-1 is probably best known for its role as an attractant of CCR2 positive cells, primarily monocytes but also basophils and certain subtypes of B- and T-cells [1–4]. By stimulating the egress of leukocytes from the bone marrow and attracting them to sites of inflammation, CCL2 is a major player in the orchestration of the immune response, as shown in various models of immunological driven pathologies [5–8]. CCL2 has been described as a selective chemokine with CCR2 as the principal receptor, which occurs as two alternatively spliced forms, CCR2a and CCR2b that differ in the C-terminus. However, the complexity of CCL2 signaling should not be underestimated because oligomerization induced by binding to glucosaminoglycans (GAG) on endothelial surfaces seems to be required for monocyte migration to sites of inflammation in vivo [9]. In addition, the dimerization of CCR2 with other chemokine receptors and the dimerization of CCL2 with other chemokines are evident although the consequences are to a great extent unknown [10,11].

Pharmacological intervention of the CCL2/CCR2 signaling has been suggested to be beneficial in treating conditions with an inflammatory component as well as malignancies. The hypothesis has been evaluated in numerous models of disease using monoclonal antibodies against both CCL2 and CCR2 as well as small molecules blocking the signaling via CCR2 [12]. A third group of molecules used to study CCL2/CCR2 biology are those derived from either CCL2 itself or from the related chemokines CCL7 (MCP-3) and CCL8 (MCP-2). This is a complex group of molecules where different functions of CCL2 have been manipulated, e.g. signaling via CCR2, GAG binding and dimerization. For example, a CCL2-P8A mutant, shown to be efficacious in a model of murine experimental autoimmune encephalomyelitis, functioned as an agonist in vitro, but was unable to participate in oligomerization on GAG [9]. In a CCL2-Y13A/S21K/Q23R triple mutant, showing efficacy in a model of experimental autoimmune uveitis, the affinity to CCR2 was reduced whereas the binding to GAG was potentiated [13].

* Corresponding author at: Swedish Orphan Biovitrum, Tomtebodavägen 23 Solna, S-112 76 Stockholm, Sweden. Tel.: +46 704107186.
E-mail address: stefan.j.svensson@sobi.com (S.S. Gelius).

0006-2952/$ – see front matter © 2011 Elsevier Inc. All rights reserved.
doi:10.1016/j.bcp.2011.12.001

Nevertheless, the majority of molecules exemplified in the literature seem to function as classical antagonists by binding to CCR2 without inducing a signaling response. Some of these, such as [5–76] CCL2 and [5–76] CCL7 are naturally occurring N-terminally truncated variants generated in vivo by matrix metalloproteinases [14–17].

The most extensively studied CCL2 variant is human [1 + 9–76] CCL2, commonly known as 7ND and was first designed by Zhang et al. [18]. 7ND has shown to be efficacious in several disease models in several species; models of cardiovascular disease, graft versus host disease, inflammation and fibrosis [19–32]. For example, it was previously described that 7ND, administered by gene transfection into skeletal muscle, is a successful therapeutic strategy against bleomycin-induced pulmonary fibrosis in mice [23]. Bleomycin is known for its pro-fibrotic effect after intratracheal administration in mice up-regulating levels of CCL2, TGF-β and extracellular matrix proteins such as collagen I, collagen III and fibronectin as well as inducing infiltration of inflammatory cells [23,33–35]. To the best of our knowledge, the actual mechanism of action of 7ND has only been studied in the context of human CCR2 and the species specificity of 7ND is poorly investigated. To better understand the properties making 7ND a powerful pharmacological tool, we decided to study the in vitro properties of 7ND in the mouse model. Here we report data that are not compatible with the picture of 7ND being a potent CCR2 antagonist but rather make us suggest that 7ND can act independently of CCR2 in mouse.

2. Material and methods

2.1. Material

The mouse CCR2-gene was co-expressed with Gα16 in CHO-A2 cells (Euroscreen S.A., Gosselies, Belgium) and maintained in UltraCHO medium (BioWittaker, Walkersville, MD, US) supplemented with 1% FBS (Gibco/Invitrogen AB, Stockholm, Sweden), 800 μg/ml Geneticin (Gibco/Invitrogen AB) and 250 μg/ml Zeocin (Gibco/Invitrogen AB) and passaged twice per week by trypsin digestion (Gibco/Invitrogen AB). THP-1 human monocyte cell line (TIB-202, ATCC/LGC, Borås, Sweden) was maintained in RPMI1640 with Glutamax (Gibco/Invitrogen AB) and 10 mM HEPES (Gibco/Invitrogen AB) and passaged twice per week. Mouse CCL2 (=JE, 479-JE/CF) was purchased from R&D Systems (Abingdon, UK). Human CCL2 was either purchased from R&D (279-MC/CF-050) or produced in-house. 7ND and Met7ND were produced in-house. The radioligand used, ^{125}I-mCCL2 (JE) was purchased from PerkinElmer (MA, US). Hank's balanced salt solution, HBSS (Gibco/Invitrogen AB) was supplemented with 20 mM HEPES, 0.04% sodium bicarbonate (Gibco/Invitrogen AB) and 0.1% BSA (Sigma–Aldrich Co, St Louis, MO, US). pH was titrated to pH 7.4 using 10 M NaOH. PBS was purchased from Gibco/Invitrogen AB.

2.2. Isolation of primary murine lung fibroblasts

Female C57BL mice (20 g) from Scanbur, Karlslunde, Denmark were group housed with ad lib access to food and water. Mice were anesthetized with a mixture of medetomidin, 0.5 mg/kg (Orion Pharma Animal Health, Sollentuna, Sweden) and ketamine, 50 mg/kg intraperitoneally (Pfizer, Sollentuna, Sverige). Eye gel, Viscotears (Novartis Healthcare, Basel, Switzerland) was administered and thereafter they were dosed intratracheally with 50 μl bleomycin, 0.6 mg/kg (Baxter, Kista, Sweden). Directly after bleomycin treatment, animals received saline, 0.5 ml subcutaneously as well as atipamezole, 1 mg/kg (Pfizer, NY, US). Mice were euthanized after 14 days. Protocols were approved by the local ethical committee (#N315/08 Stockholm north). Whole lungs from single animals were cut into small pieces and placed in 40 ml media, DMEM with Glutamax (Gibco/Invitrogen AB), 10% FBS and 1% penicillin/streptomycin (Gibco/Invitrogen AB) in 160 cm^2 tissue culture plates. Lung tissue cells were incubated at 37 °C in a humidified atmosphere (5% CO_2) and when the cells reached 70% confluence they were passaged using trypsin digestion.

2.3. Collagen I immunostaining of murine fibroblasts

Murine fibroblasts were plated in poly-D-lysine/laminine coated 8-well slides (Becton Dickinsson, Stockholm, Sweden); 10,000 cells per well in culture medium and incubated at 37 °C in a humidified atmosphere (5% CO2) overnight. Cells were washed with PBS and fixed in paraformaldehyde (Sigma–Aldrich), 4% in PBS. After 15 min, cells were washed and permeabilized in 0.5% TritonX-100 (Sigma–Aldrich)/PBS for 10 min. Cells were then incubated with rabbit-anti-mouse collagen 1 antibodies (Cedarlane Labs, Nordic BioSite AB, Täby, Sweden), diluted 1:20 in PBS and incubated at room temperature for 1 h. After three washes with PBS, cells were incubated with goat-anti-rabbit-FITC antibodies (R&D Systems, Abingdon, UK), diluted 1:20 for 40 min. Staining was visualized using a fluorescence microscope (Leica DM IRB, Kista, Sweden). Cells stained with only the goat-anti-rabbit antibody was used as a negative control.

2.4. Cloning and expression of Met7ND, 7ND and murine CCR2

A synthetic gene coding for 7ND, [1 + 9–76] CCL2 with a human CCL2 signal peptide sequence (GenBank NM_002982) was ordered from Geneart AG (Life Technologies, NY, US). The synthetic gene was inserted into the pcDNA3.1(+) expression vector (Invitrogen AB). Protein expression was performed using the FreeStyle™ 293 Expression System (Invitrogen AB). The expression vector for human CCL2 (GenBank NP_002973) was created by constructing a DNA sequence coding for MASHHHHHHASGDYKDDDDK-CCL2 (residues 24–99) using the synthetic gene described above as PCR template followed by insertion into the pET-21d(+) expression vector (Novagen, Solna, Sweden). Cloning of correct sequence was verified by DNA sequencing. Expression of the 6xHis and FLAG peptide tagged CCL2 was performed in *Escherichia coli* BL21-AI cells (Invitrogen AB) essentially as recommended by the suppliers. The expression vector for Met7ND was created using the synthetic gene described above as PCR template followed by insertion into the pET-21b(+) expression vector (Novagen) and verification by DNA sequencing. Expression was performed in *E. coli* BL21-AI cells essentially as recommended by the suppliers. The gene coding for mouse CCR2 (GenBank NM_009915) was isolated from mouse brain cDNA by PCR amplification and inserted into the pcDNA3.1(+) expression vector. Cloning of correct sequence was verified by DNA sequencing. Protein production was performed in stably transfected CHO-A2 Gα16 cells (Euroscreen S.A.).

2.5. Purification of recombinant proteins

Medium containing 7ND was filtered through a Sartolab P plus (Sartorius, Fisher Scientific, Västra Frölunda, Sweden), 0.2 μm before capturing 7ND on a HiTrap SP HP column (GE Healthcare, Uppsala, Sweden) equilibrated with 20 mM sodium phosphate, pH 7.0. 7ND was eluted by a 0–0.6 M NaCl gradient. 7ND containing fractions where purified further using size exclusion chromatography on a Superdex 75 column (GE Healthcare).

Human CCL2 was purified from *E. coli* inclusion bodies. The cell lysate was centrifuged at 10,000 × *g* for 20 min and the pellet (5 g) was resuspended and washed twice in 25 ml 25 mM sodium phosphate (Sigma–Aldrich), 0.25% sodium deoxycholate (Merck AB, Solna, Sweden) pH 7.5 and twice in 25 ml 25 mM sodium

phosphate, pH 7.5. The final pellet was resuspended and solubilized with 4 ml of 6 M Guanidine HCl (Sigma–Aldrich). CCL2 was refolded by rapid dilution in 400 ml 100 mM Tris–HCl (Sigma–Aldrich), 0.2 mM GSSG (Sigma–Aldrich), 1 mM GSH (Sigma–Aldrich), pH 8.0 and incubated at 4 °C for 17 h. CCL2 was further purified by ion exchange chromatography on a HiTrap SP HP column using a NaCl gradient in 20 mM sodium phosphate, pH 7.0. The pooled fractions were submitted to buffer exchange on a PD-10 column (GE Healthcare) equilibrated with 50 mM Tris pH 8.0, 1 mM $CaCl_2$ (Sigma–Aldrich) and 0.1% Tween20 (Sigma–Aldrich). The sample was then incubated with 23 U enterokinase/mg total protein (EKMax, Invitrogen AB, Stockholm, Sweden) at 4 °C for 17 h. CCL2 was finally separated from the cleaved 6xHis/FLAG-tag by repeating the ion exchange chromatography step followed by size exclusion chromatography on a Superdex 75 column. Met7ND was prepared from *E. coli* inclusion bodies and isolated by ion exchange chromatography on a HiTrap SP HP column followed by size exclusion chromatography on a Superdex 75 column, essentially as described for human CCL2.

Protein quality was assessed by SDS-PAGE, MALDI-TOF MS and N-terminal sequencing. All proteins where purified to apparent homogeneity. N-terminal protein sequencing using Edman degradation of the proteins was performed with a Procise HT Sequencing system (Applied Biosystems, Stockholm, Sweden). The samples were sequenced using a pulsed liquid PVDF method. The proteins were loaded and sequenced before and after digestion with pyroglutamate amino peptidase (Sigma–Aldrich) in order to deblock the N-terminus. Molecular masses of the proteins were measured using a Voyager DE-STR MALDI-TOF mass spectrometer (AB SCIEX, Stockholm, Sweden).

2.6. CCR2-mediated calcium release

Measurement of CCL2 stimulated calcium release in THP-1 cells and mouse CCR2 overexpressing CHO-A2 cells were performed using HitHunter Calcium NoWash Kit (DiscoveRx, Birmingham, UK) according to the instructions provided by the manufacturer.

Briefly, THP-1 cells, cultivated in RPMI1640 with Glutamax, 10% FBS and 10 mM HEPES were washed once in PBS and plated in 96-well microplates (3603 Costar, Sigma–Aldrich, Stockholm, Sweden), 200,000 cells/well in 50 μl and incubated for 1 h in humidified atmosphere (5% CO_2) at 37 °C. 2× dye (50 μl) was added to each well and incubation was repeated for 1 h.

CHO-A2 cells stably expressing mouse CCR2 and Gα16 were plated at a cell density of 30,000 cells/well in 96-well microplates (3603 Costar) and incubated overnight in humidified atmosphere (5% CO_2) at 37 °C. Medium was removed and cells were stained according to the instruction of the manufacturer. Incubation was repeated for 50 min.

In FLIPR96 (Molecular Devices, Sunnyvale, CA, US) cells were co-incubated with either 4 nM hCCL2 or 1.5 nM mouse CCL2 final concentrations and 7ND ranging from 3 μM to 17 pM final concentrations while changes in cytosolic calcium were measured. Maximum emission data from each well were collected and inhibition of the response, fKi elicited by 4 nM hCCL2 or 1.5 nM mouse CCL2 by 7ND was calculated. fKi was defined as:

$$\text{fKi} = \frac{\text{IC50}}{(1 + (\text{challenge dose of agonist}/\text{EC50 of agonist}))}$$

2.7. Chemotaxis assay

Cell migration of THP-1 cells was determined using Transwell 96-well microplates of 5 μm pore size (Corning, VWR, Stockholm, Sweden). Assay buffer (150 μl), HBSS with 0.1% BSA, with or without human CCL2 (3 nM) was added to the lower chambers. 7ND (50 μl) at concentrations between 0.1 and 1000 nM or buffer, resuspended with cells (10^6 cells/ml) was added to the filter inserts (upper chamber) and cells were allowed to migrate for 4 h in humidified atmosphere (5% CO_2) at 37 °C. The fraction of cells that migrated to buffer represented spontaneous migration. Control experiments were made for measurements of the intrinsic chemotactic effect of 7ND by placing 7ND (0.1–1000 nM) in the lower wells and cells and buffer in the filter inserts, allowing cells to migrate for 4 h at the previous conditions. For quantification, migrated cells were stained in 2 μM Calcein-AM (Gibco/Invitrogen AB) for 1 h and absorbance at 495/520 was monitored using Envision 2102 multilabel reader (PerkinElmer).

2.8. Radioligand binding

CHO cells stably expressing mouse CCR2 and Gα16 were plated 24 h prior to the experiment in 96-well plates (Costar) at a density of 50,000 cells/well. The saturation experiment was performed in a final volume of 200 ml binding buffer, HBSS supplemented with 0.1% BSA, with serial dilutions of radio ligand ^{125}I-JE. Nonspecific binding was defined as the amount of radio activity remaining bound to the cells after incubation in the presence of 100 nM unlabeled mCCL2. Displacement experiments were performed in binding buffer with various concentrations of the peptides mCCL2 (JE), hCCL2 or 7ND included in the incubation mixture together with 40–70 pM ^{125}I-JE. The plate was incubated for 1 h at 37 °C and 5% CO_2. Incubation was terminated by aspiration of the radioligand mix using an 8-channel vacuum manifold followed by manual addition of 100 μl ice cold 50 mM Tris buffer. Washing was repeated twice. Microscint20 (100 μl) (PerkinElmer) was added to each well and the radioactivity was counted using a Wallac 1450 Trilux 32 counter (PerkinElmer). Non-linear regression calculations were performed using Excel with XLfit 5 plugin.

2.9. Kinetic determinations by using surface plasmon resonance, SPR

Purified mouse CCL2 was immobilized on a CM1 sensor chip (GE Healthcare) by amine coupling at a low density of 220 Ru (about 0.22 ng/mm^2) mCCL2 to determine kinetics of 7ND and Met7ND binding using a Biacore 2000 (GE Healthcare). BSA was immobilized on the same chip and was used as a reference surface. 7ND at concentrations from 2.3 nM up to 3.6 μM and Met7ND at concentrations from 0.9 μM up to 3.6 μM were passed over the sensor chip at a flow rate of 20 μl/min. Each kinetic determination was performed at least at eight different concentrations with one point in duplicate. The BIAevaluation software (GE Healthcare) was used for analysis of the association and dissociation profiles of the sensorgrams. Interaction constants were determined by performing non-linear fitting of data, corrected for bulk refractive index changes, according to one or two-site models.

2.10. Stimulation of primary murine lung fibroblasts

Primary murine lung fibroblasts were plated in 24-well plates (Costar), 50,000 cells/well in DMEM with Glutamax, 10% FBS and 1% penicillin/streptomycin and incubated overnight in humidified atmosphere (5% CO_2) at 37 °C. Cells were starved for 24 h in DMEM with Glutamax, 1% penicillin/streptomycin and 0.5% BSA (fatty acid free, Sigma A8806) prior to stimulation with 7ND diluted in starvation medium (0, 0.01, 0.1 and 1 nM). After 24 h stimulation, supernatants were collected, cells were washed once with PBS, and lysed using lysis buffer (RNeasy Mini Kit, Qiagen, Sollentuna, Sweden) supplemented with 1% β-mercaptoethanol (Sigma–Aldrich) and stored at −70 °C. Stimulation experiments were performed on three occasions using isolated fibroblasts from

different mice. A potential 7ND-induced apoptosis of murine fibroblasts was analyzed using Guava TUNEL Kit and measured in Guava Easy Cyte (Millipore, Solna, Sweden). Fibroblasts, starved for 24 h, were incubated with 10 nM 7ND for 24 h and analyzed for number of apoptotic cells compared with unstimulated cells (negative control) and cells stimulated with 100 μM cycloheximide (Millipore, positive control).

2.11. Analysis of secreted proteins, fibronectin, CCL2 and collagen I

Murine fibronectin and CCL2 secreted from 7ND-stimulated lung fibroblasts were analyzed using ELISA kits, Murine fibronectin (Kamiya Biomedical Company, Seattle, WA, US) and Murine CCL2 (Thermo Scientific, Stockholm, Sweden) according to instructions provided by the manufacturer.

Collagen type I secretion was assessed by Western blotting. Medium was reduced and incubated at 85 °C before loading on a NuPAGE 4–12% gel (Invitrogen, Stockholm, Sweden). Protein was wet transferred to a PVDF membrane (BioRad, Sundbyberg, Sweden) that was subsequently blocked with 5% BSA. Membranes were incubated with purified rabbit anti-mouse collagen type I polyclonal antibody diluted 1:1000 (Cederlane Labs CL50151AP, Nordic BioSite AB, Täby, Sweden) followed by incubation with HRP conjugated anti rabbit antibody diluted 1:3000 (Dako, Glostrup, Denmark) and developed using ECL Plus (GE Healthcare). Intensity of immunoreactive bands was quantified using a LAS-3000 CCD camera (R&D Systems) and the accompanying software package.

2.12. mRNA expression analyses by real time-PCR

Total RNA isolation from cells was performed using RNeasy Micro Kit (Qiagen) and quantified by absorbance at 260 nm followed by capillary electrophoresis on Agilent Bioanalyzer Lab On Chip (Agilent Technologies, Kista, Sweden) for quality control. cDNA synthesis was performed with 100–200 ng of total RNA from each sample using High Capacity cDNA archive kit (Applied Biosystems, Stockholm, Sweden) with thermal cycling conditions; 25 °C for 10 min, 37 °C for 120 min and 85 °C for 10 s. To exclude the possibility of genomic DNA contamination, all samples were also treated the same way in the absence of Reverse Transcriptase. RT-PCR was performed using TaqMan® Gene Expression Master Mix and Gene Expression Assays (Applied Biosystems). Assay IDs were from Applied Biosystems: mouse collagen type I (Mm00801666_g1), mouse collagen type III (Mm00802331_m1) and mouse α-SMA (Mm01204962_gH). Each sample was analyzed in duplicate, with each reaction using 1 ng of cDNA in a total reaction volume of 10 μl. Thermal cycling conditions were 50 °C for 2 min, 95 °C for 10 min, 40 cycles of 95 °C for 15 s and 60 °C for 1 min using the 7900HT Sequence Detection Systems (Applied Biosystems). No PCR product was detected in the procedure without reverse transcriptase. The amount of target, normalized to 18S rRNA (endogenous reference) and relative to a calibrator (unstimulated samples), is reported as $2^{-\Delta\Delta CT}$, which gives the relative quantification of gene expression.

3. Results

3.1. 7ND inhibits CCL2-stimulated calcium release and chemotaxis in the human THP-1 monocyte cell line

7ND was produced in HEK293 cells and purified to homogeneity. Roughly 50% of the protein was glycosylated at Asn14, and the N-terminus harbored the pyroglutamate modification previously described for full length CCL2 [36]. The function of 7ND was characterized in human monocytes. The THP-1 monocyte cell line was chosen as this cell line endogenously expresses CCR2b and is responsive to human CCL2. In our experiments, human CCL2 stimulated calcium release with a pEC_{50} of 8.50 ± 0.35 (3.2 nM). This is in agreement with data previously reported [37]. The in house refolded *E. coli* produced CCL2 was equipotent with the commercially *E. coli* produced CCL2 (data not shown).

Inhibition of CCL2-mediated calcium release mediated by 7ND was determined in the range of 17 pM to 1 μM with an hCCL2, EC_{70} challenge dose of 4 nM. As shown in Fig. 1A, 7ND inhibited CCL2 stimulated calcium release in THP-1 cells with a pfKi value of 7.53 ± 0.21 (29 nM). 7ND did not show any calcium stimulating effect on its own (data not shown).

Inhibition of CCL2 stimulated chemotaxis was studied using the THP-1 cells in a Transwell migration assay. Human CCL2 stimulated migration with an EC_{50} of 2 nM and an EC_{70} challenge dose of 3 nM was chosen to study 7ND inhibition. Results, illustrated in Fig. 1B, show that 50% of the cells were inhibited from migrating at approximately 100 nM while >90% of the cells were inhibited from migrating by 1 μM 7ND. 7ND itself was a weak inducer of migration of THP-1 cells and elicted a maximal response (7ND > 30 nM) that was 30% of the maximal CCL2 response.

3.2. 7ND is a low potency antagonist of the CCL2/CCR2 interaction in mouse.

The interaction of 7ND with mouse CCR2 was studied in a stably transfected CHO cell line expressing Gα16 and CCR2. Expression of mouse CCR2 was confirmed by RT-PCR and cells were shown to give a cytosolic calcium release in response to mCCL2. The pEC50 for mCCL2 was determined to 8.76 ± 0.24 (2 nM). Non-transfected CHO cells did not respond to mCCL2. A challenge dose of 1.5 nM mCCL2 was used to study inhibition of calcium release by 7ND. At 1 μM of 7ND, 40–80% of the calcium release elicited by 1.5 nM mCCL2, was inhibited ($n = 6$, data not shown). 7ND showed no agonistic effects on calcium release in mouse CCR2-transfected cells (data not shown).

7ND binding to mouse CCR2 was studied using a displacement assay with ^{125}I-labeled mouse CCL2. The saturation analysis supported a single site model for ^{125}I-JE binding to CHO cells stably expressing the mouse CCR2 with a K_D of 290 pM and an estimated receptor density of 31,000 receptors/cell (assuming 50,000 cells/well as plated initially, $n = 1$). The three peptides mCCL2, hCCL2 and 7ND displaced ^{125}I-mCCL2 with pK_i values of 9.33 ± 0.22 (0.46 nM), 7.22 (60 nM,) and >6 (>1 μM), respectively with Hill coefficients close to unity demonstrated in Fig. 2. From these results we could conclude that there is a significant species barrier in terms of displacing CCL2 from CCR2 and that 7ND is a low potency inhibitor of the CCL2/CCR2 interaction in mouse.

3.3. Interaction between mouse CCL2 and 7ND

In order to study the interaction between 7ND and mCCL2, we immobilized mCCL2 and studied binding kinetics by SPR. Use of the standard Biacore sensor chips (CM5 carboxy methylated dextran) resulted in high degree of non-specific binding of all CCL2 ligands, probably due to interactions with the dextran matrix of the chip. Therefore, the C1 chip (dextran free) was chosen and virtually no response was detected on reference surfaces when injecting 7ND. Recorded sensorgrams over a wide range of concentrations showed that 7ND binds mouse CCL2 (Fig. 3A). The single step one-site binding model could not be satisfactory fitted to the sensorgrams and multiple parameter fitting was evaluated. A one site binding model including an isomerization step was best fitted to the data ($A + B \leftrightarrow AB \leftrightarrow AB^*$, Fig. 3A). The dissociation constant of the 7ND/mCCL2 complex was determined to 670 nM. In contrast, Met7ND showed no specific binding to mouse CCL2 (Fig. 3B).

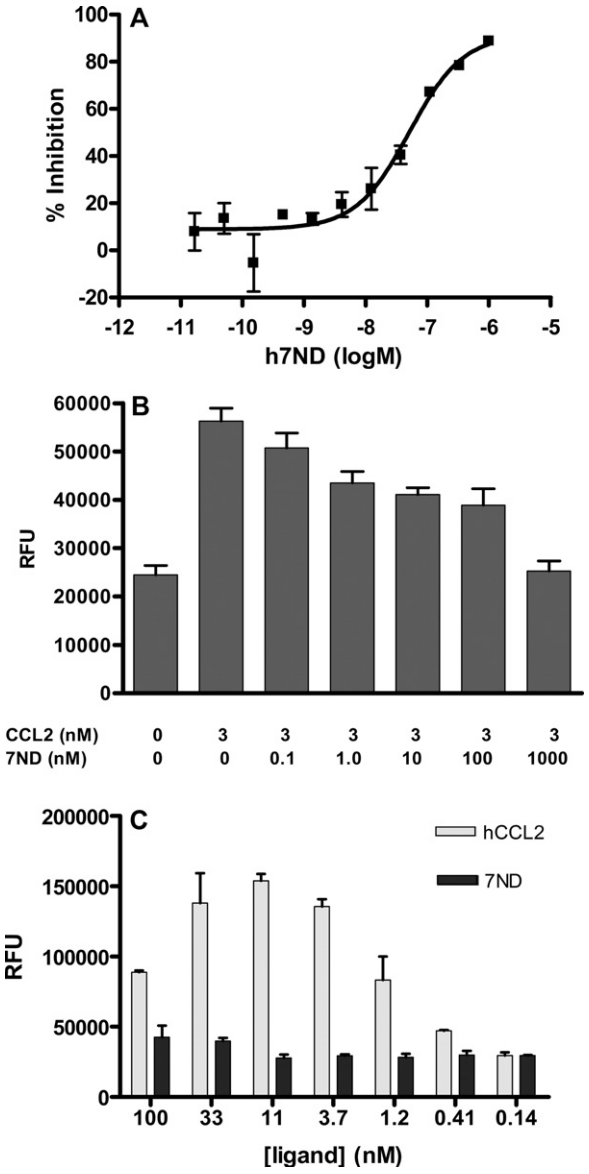

Fig. 1. 7ND mediated inhibition of human CCL2 stimulated cytosolic calcium release and cell migration of THP-1 cells. (A) Human monocyte cell line THP-1 was co-stimulated with a challenge dose of 4 nM human CCL2 ($\approx EC_{70}$) and 7ND at different concentrations. Cytosolic calcium release was measured and plotted as % inhibition of the response elicited by 4 nM human CCL2. 7ND inhibited CCL2-stimulated calcium release with a pfKi value of 7.53 ± 0.21 (29 nM, $n = 3$). (B) Inhibition of CCL2-induced cell migration by 7ND was determined using Transwell 96-well microplates of 5 μm pore size. Human CCL2 (150 μl), 3 nM ($\approx EC_{70}$ challenge dose) or buffer was added to the lower chambers. 7ND (50 μl) at concentrations between 0.1 and 1000 nM or buffer, resuspended with THP-cells (10^6 cells/ml) were added to the upper chambers and allowed to migrate for 4 h in humidified atmosphere (5% CO_2) at 37 °C. Relative fluorescence (RFU), as a measure of migrated cells, was plotted as a function of 7ND concentration ($n = 3$). (C) Control experiments were made for measurements of the chemotactic potency of 7ND and human CCL2 by placing ligands at different concentrations or buffer in the lower wells and THP-1 cells and buffer in the filter inserts, allowing cells to migrate for 4 h in humidified atmosphere (5% CO_2) at 37 °C. Cells found in lower wells with buffer represented spontaneous migration. Relative fluorescence (RFU), as a measure of migrated cells was plotted as a function of CCL2 and 7ND concentration.

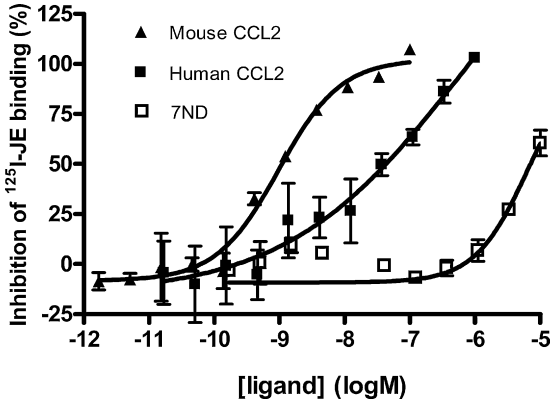

Fig. 2. Displacement of ^{125}I-JE binding to mouse CCR2. CHO cells stably expressing mouse CCR2 and Gα16 were plated in 96-well plates at a density of 50,000 cells/well. Displacement experiments were performed in binding buffer with various concentrations of the peptides mCCL2 (JE), hCCL2 and 7ND included in the incubation mixture together with 40–70 pM ^{125}I-JE. The three peptides mCCL2, hCCL2 and 7ND displaced ^{125}I-mCCL2 with pK_i values of 9.33 ± 0.22 (0.46 nM, $n = 4$), 7.22 (60 nM, $n = 1$), and >6 (>1 μM, $n = 4$), respectively. Nonspecific binding was defined as the amount of radio activity remaining bound to the cells after incubation in the presence of 100 nM unlabeled mCCL2.

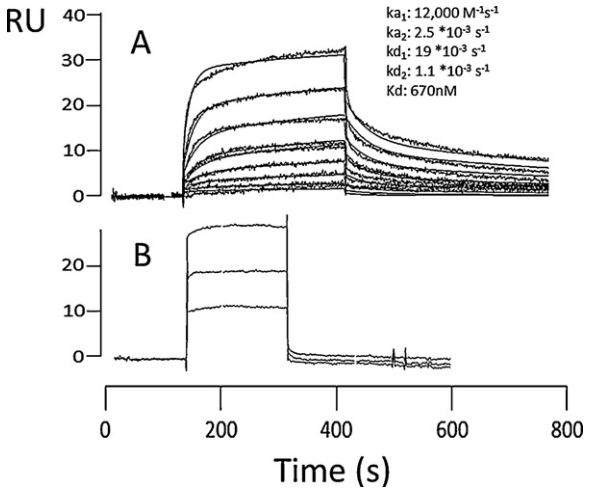

Fig. 3. 7ND binds mouse CCL2 immobilized on a Biacore CM1 sensor chip. (A) 7ND, at concentrations from 2.3 nM up to 3.6 μM, was passed over the ship. Sensorgrams were recorded and a one site binding model including an isomerization step was fitted to the data ($A + B \leftrightarrow AB \leftrightarrow AB^*$). (B) Met7ND (7ND produced in *E. coli* harboring a start codon methionine and no pyroglutamate modification) sensorgrams at 0.9, 1.8 and 3.6 μM, showing no specific binding.

3.4. 7ND mediates anti-fibrotic effects on murine lung fibroblasts via a pathway distinct from CCR2

In order to investigate the mechanism of which 7ND mediates its anti-fibrotic effects in mice, we used fibroblasts isolated from bleomycin-induced mice. During the first seven days, cells with a spider-like morphology were observed, indicating growth of fibrocytes [38]. After 11–14 days, cells turned more spread-out and transparent, a morphology associated with activated fibroblasts. Cells were labeled with an anti-mouse collagen I antibody, stained with a FITC-conjugated secondary antibody and analyzed using fluorescence microscopy. By image visualization it was estimated that more than 95% of the cells were positive for collagen type I, (Fig. 4). Significant mRNA expression levels of fibrosis markers; fibronectin, collagen I, collagen III, α-SMA and TGF-β1 were detected which strongly indicates that the main cell population was fibroblasts [39,40]. Fibroblasts, cultivated for 11 days and starved in serum-free medium were stimulated with 7ND (0, 0.01, 0.1 and 1 nM) to investigate if 7ND was capable to affect basal levels of pro-fibrotic markers.

Using TUNEL assay it was shown that stimulation with 7ND (10 nM) for 24 h in starvation medium, did not induce apoptosis of murine lung fibroblasts (data not shown).

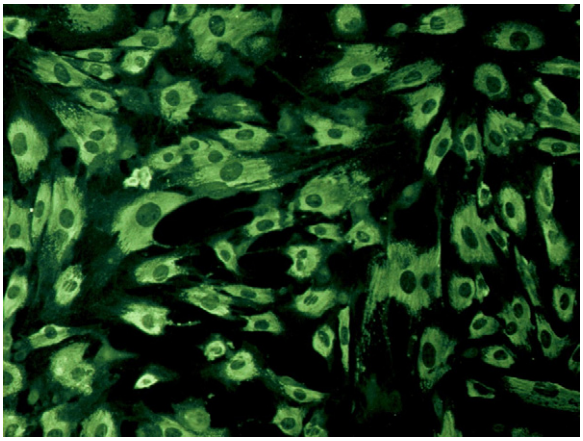

Fig. 4. Collagen I immunostaining of murine fibroblasts. Expression of collagen I in primary mouse fibroblasts visualized by immunostaining using a rabbit-anti-mouse Col 1 and goat-anti-rabbit-FITC antibodies followed by fluorescence microscopy. Cells were examined at 40× magnification.

3.4.1. 7ND inhibits synthesis of extracellular matrix proteins in murine lung fibroblasts

Levels of secreted fibronectin were significantly decreased by 7ND in a concentration dependent manner (Fig. 5A). While unstimulated fibroblasts secreted 2400 ng fibronectin/ml, cells stimulated with 1 nM 7ND secreted 950 ng/ml. At this time-point (24 h post-stimulation) the mRNA expression of fibronectin was not effected by 7ND stimulation (data not shown). As assessed by Western blot using an anti-collagen I antibody, the levels of secreted collagen I were significantly decreased with increased concentrations of 7ND (Fig. 5B). Levels of collagen I secreted from fibroblasts stimulated with 1 nM 7ND were one third of those secreted from un-stimulated cells. In accordance with this 7ND also mediated inhibition of collagen I mRNA expression following the same pattern as for secreted collagen I protein. Cells stimulated with 1 nM 7ND expressed 60% of the collagen I mRNA expressed in un-stimulated cells as shown in Fig. 6A. Collagen III, another collagen subtype associated with fibrotic tissue was expressed at significant levels as well by the fibroblasts. Inhibition of collagen III mRNA expression was significant in cells stimulated with 1 nM 7ND, expressing 70% of collagen III mRNA compared with un-stimulated cells as shown in Fig. 6B.

3.4.2. Fibroblasts isolated from bleomycin-treated mice express CCL2, TGF-β and α-SMA mRNA but not significant levels of CCR2

One distinction between fibrocytes (CCR2 positive) and fibroblasts (CCR2 negative) is related to expression of CCR2. It has been shown that mesenchymal cells isolated from mouse lung transform to fibroblasts with time, and that the major shift appears during day 7–11 in culture [38]. In agreement with this observation, our cells, after 11 days in vitro, expressed significant levels of collagen I but no significant levels of CCR2 (data not shown).

Expression of CCL2, TGF-β and α-SMA is associated with a pro-fibrotic phenotype of activated fibroblasts [41]. Inhibition of CCL2 secretion was significant in cells stimulated with 1 nM 7ND, secreting 75% of CCL2 compared with un-stimulated cells (Fig. 5C). At this time-point the mRNA expression of CCL2 was not effected by 7ND stimulation (data not shown). TGF-β, an important pro-fibrotic factor promoting proliferation of fibroblasts and differentiation of fibroblasts to myofibroblasts was detected at significant mRNA expression levels at the time-point of interest (data not shown). Inhibition of α-SMA mRNA expression was significant in cells stimulated with 0.1–1 nM 7ND, expressing 60% of α-SMA mRNA at 0.1 nM 7ND and 50% at 1 nM 7ND compared with un-stimulated cells presented in Fig. 6C.

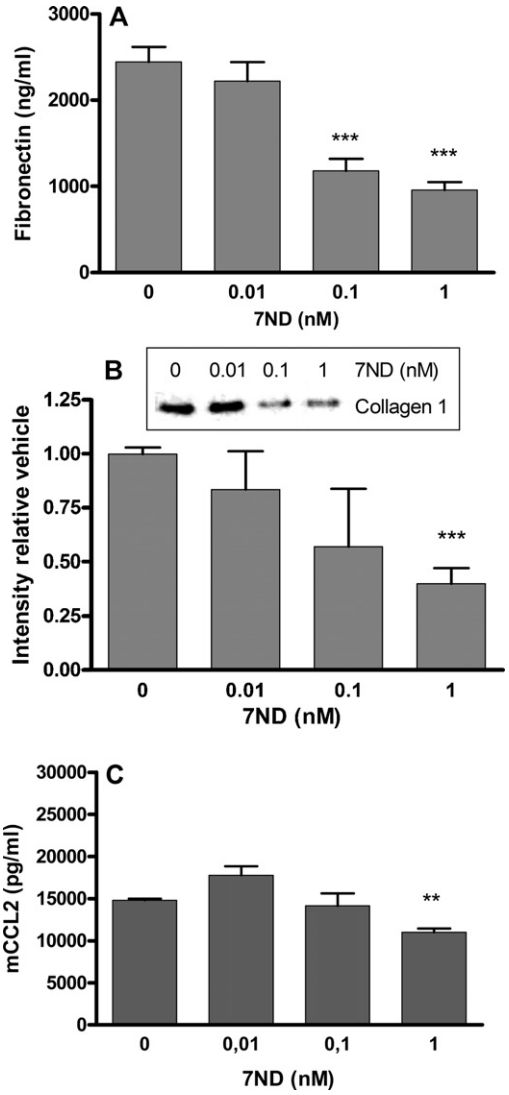

Fig. 5. 7ND inhibits secretion of extracellular matrix proteins from murine lung fibroblasts in a concentration dependent manner. Cells were isolated from whole lungs after 14 days single dose treatment of 0.6 mg/kg bleomycin, and cultured for 11 days followed by 7ND stimulation. (A) Fibronectin concentration analyzed with ELISA, (B) collagen type I analyzed with Western Blot, (C) CCL2 analyzed with ELISA. Graphs indicate data from one representative experiment ($n = 3$). Data are presented as mean + SEM. $^{*}P < 0.05$, $^{**}P < 0.01$, $^{***}P < 0.005$.

The results indicate that 7ND may inhibit differentiation of fibroblasts to myofibroblasts.

4. Discussion

The truncated form 7ND, [1 + 9–76] CCL2 has been characterized in a number of animal models of cardiovascular disease, graft versus host disease, inflammation and fibrosis. Although it is generally assumed, there are no data showing that 7ND is acting by a mechanism involving CCR2 in these models. In the reported in vivo studies, 7ND has been given as gene therapy, typically resulting in plasma levels comparable to those of endogenous CCL2, i.e. in the low picomolar range. The majority of studies have been performed in mice, but studies in rat, rabbit and monkey models have been reported too [19,22]. Here we show that 7ND is a low-potency antagonist in vitro as micromolar concentrations are needed to effectively inhibit CCL2 signaling via mouse CCR2. Thus, the in vitro potency is roughly four orders of magnitude lower than what would be expected from the in vivo studies. This

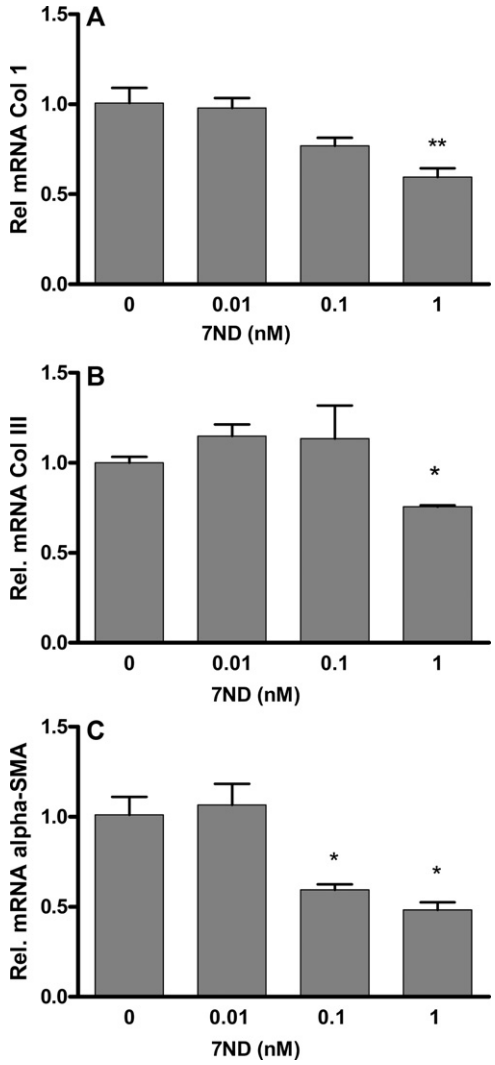

Fig. 6. 7ND inhibits mRNA expression levels of fibrotic markers in murine lung fibroblasts in a concentration dependent manner. Cells were isolated from whole lungs after 14 days single dose treatment of 0.6 mg/kg bleomycin, and cultured for 11 days followed by 7ND stimulation. Levels of mRNA transcripts were detected by real-time PCR. (A) Collagen I, (B) collagen III, (C) α-smooth muscle actin. Representative data of 1 of 3 experiments are presented and values are the mean + SEM. $^{*}P < 0.05$, $^{**}P < 0.01$, $^{***}P < 0.005$.

makes us suggest that CCR2 antagonism is most probably not the mechanism of 7ND action.

Next we asked ourselves if 7ND possibly could interfere with endogenous CCL2 signaling by dimerization. The classical interpretation of the displacement data generated with ^{125}I mCCL2 is that 7ND functions as a competitive inhibitor on murine CCR2 but an alternative interpretation would be that 7ND functions as a dominant negative inhibitor, by forming a non-signaling heterodimer with mCCL2. It is well documented that chemokines can undergo dimerization, both as homo- and heterodimers. The homodimer seen in crystal structures of human CCL2, is formed by an antiparallel beta-sheet involving Val9 to Cys11 in both subunits [42]. This suggests that dimerization is inhibitory, as the dimer interface engage residues important also for receptor binding. Our data clearly show that 7ND can bind mouse CCL2 although further studies of the 7ND/mCCL2 complex in solution is required to shed light on the stoichiometry. In contrast to the 7ND produced in mammalian cells, 7ND produced in *E. coli* (Met7ND) did not bind mouse CCL2. The structural differences between these proteins are found in the N-terminus as *E. coli* production introduces a start codon methionine, which in turn prevents pyroglutamate formation of the initial glutamine. These data indicate that the N-terminus is important for the 7ND/mCCL2 binding and agree with the binding epitope seen in the CCL2 crystal structure where Pro8 is positioned in a groove formed by residues from the opposing subunit (Thr10, Ile42, Arg29, Glu50, Cys12 and Cys52). A 7ND/mCCL2 heterodimer interface would align the N-terminal pyroglutamate residue of 7ND in the same pocket as Pro8 of full-length CCL2 and allow the same kind of interactions. The importance of Pro8 in heterodimerization has elegantly been established by Paavola et al. [43] by showing that the P8A mutant does not form dimers. Although the weak interaction between 7ND and mouse CCL2 may not be of pharmacological significance, it is interesting to note that it is of the same order of magnitude as the K_i value obtained from the displacement studies of mCCL2 from membrane preparations with over expressed mouse CCR2. These results make us suggest that 7ND possibly could function as a low potency antagonist of mouse CCL2/CCR2 signaling by dominant negative 7ND/CCL2 dimerization.

With the results suggesting that CCR2 inhibition is of minor importance for the 7ND activity in mouse, we next searched for a CCR2 devoid ex vivo system to evaluate 7ND potency. We decided to focus on its potential role in fibrosis as it has been reported that CCL2 not only promotes recruitment of immune cells such as monocytes and fibrocytes to sites of experimentally induced fibrosis, but also modulates fibroblast properties [41]. The potential anti-fibrotic role of 7ND was therefore studied on lung fibroblasts isolated from bleomycin-induced fibrotic mice. Intratracheal administration of bleomycin in mice is an established in vivo fibrosis model resulting in acute lung injury, inflammation and extracellular matrix deposition [23]. Beside modulation of collagen expression, we observed 7ND mediated down regulation of fibronectin, a glycoprotein known to mediate attachment of fibroblasts to extracellular matrix in fibrotic lungs [44]. 7ND also inhibited α-SMA expression. Taken together, our in vitro observations illustrate the anti-fibrotic properties of 7ND and suggest a role of 7ND in attenuation of differentiation/activation of fibroblasts to myofibroblasts.

Although there are examples where CCR2 expression has been detected in fibroblasts, e g fibroblasts explanted from skin of scleroderma patients [45], the fact that no significant expression of CCR2 was detected in our fibroblasts agrees well with data previously reported [38,46]. Moore et al. [38] described that CCR2 knock-out mice were protected from FITC-induced lung fibrosis in comparison with the wild-type. This role of CCR2 could be linked to fibrocyte infiltration, as fibrocytes, isolated from lungs of FITC-induced wild-type mice were characterized not only by expression of CD45 and type I collagen but also by expression of CCR2. After 7 days in culture the fibrocytes had lost their CD45 expression as well as expression of the CCR2 receptor but were still positive for collagen 1. It was suggested that fibrocytes had transformed to mature fibroblasts, typically positive for collagen I but not for CD45 or CCR2.

Further studies are needed to define the receptor and the downstream signaling pathway by which 7ND mediates its anti-fibrotic effects on fibroblasts. In this context it is interesting to note that recent studies pointed out the cytokines interferon-γ, interferon-β, IL-1α and IL-1β as mediators of similar anti-fibrotic effects in cultured fibroblasts [47–49]. A common denominator for cytokine stimulation of fibroblasts seemed to be the up-regulation of CCAT/enhancer-binding protein β (CEBP/β), a transcription factor which binds the promoters of the α-SMA, Col1A2 and fibronectin genes and thereby suppresses their transcription. Although this is the first report of CCR2 independent effects of 7ND, it should be pointed out that such effects have been reported for full-length CCL2 as well. Hepatic stellate cells chemotaxis was shown to be

induced by CCL2 in the absence of CCR2 receptor, a response that was accompanied by cytosolic calcium release, PI3-K activity and protein tyrosine phosphorylation [50]. Another study described CCL2 mediated up-regulation of tissue factor activity in aortic smooth muscle cells isolated from CCR2 knock-out mice mediated by Gαi, calcium release and mitogen-activated protein kinases p42/44 [51]. These studies indicate a role of CCL2 in the pathology of fibrosis that is not entirely dependent on CCR2. Thus, a possible hypothesis is that the CCL2/CCR2 axis is important for the recruitment of inflammatory cells to the alveolar space in response to fibrotic injury, but once the cells are in place the function of CCR2 is not essential. Instead other pathways, where 7ND is pharmacologically active, come into play.

5. Conclusions

In this study we have shown that 7ND inhibits activation of mouse lung fibroblasts independently of CCR2. Our data also point out that 7ND is a weak antagonist of the mouse CCL2/CCR2 interaction. Our conclusion from these data is that the previously reported effects of 7ND in murine disease models are most likely not mediated via the CCR2 receptor.

References

[1] Deshmane SL, Kremlev S, Amini S, Sawaya BE. Monocyte chemoattractant protein-1 (MCP-1): an overview. J Interferon Cytokine Res 2009;29:313–26.
[2] Bischoff SC, Krieger M, Brunner T, Rot A, von Tscharner V, Baggiolini M, et al. RANTES and related chemokines activate human basophil granulocytes through different G protein-coupled receptors. Eur J Immunol 1993;23: 761–7.
[3] Carr MW, Roth SJ, Luther E, Rose SS, Springer TA. Monocyte chemoattractant protein 1 acts as a T-lymphocyte chemoattractant. Proc Natl Acad Sci USA 1994;91:3652–6.
[4] Valente AJ, Graves DT, Vialle-Valentin CE, Delgado R, Schwartz CJ. Purification of a monocyte chemotactic factor secreted by nonhuman primate vascular cells in culture. Biochemistry 1988;27:4162–8.
[5] Shahrara S, Proudfoot AE, Park CC, Volin MV, Haines GK, Woods JM, et al. Inhibition of monocyte chemoattractant protein-1 ameliorates rat adjuvant-induced arthritis. J Immunol 2008;180:3447–56.
[6] Crane MJ, Hokeness-Antonelli KL, Salazar-Mather TP. Regulation of inflammatory monocyte/macrophage recruitment from the bone marrow during murine cytomegalovirus infection: role for type I interferons in localized induction of CCR2 ligands. J Immunol 2009;183:2810–7.
[7] Nakajima H, Kobayashi M, Pollard RB, Suzuki F. Monocyte chemoattractant protein-1 enhances HSV-induced encephalomyelitis by stimulating Th2 responses. J Leukoc Biol 2001;70:374–80.
[8] Takahashi M, Galligan C, Tessarollo L, Yoshimura T. Monocyte chemoattractant protein-1 (MCP-1), not MCP-3, is the primary chemokine required for monocyte recruitment in mouse peritonitis induced with thioglycollate or zymosan A. J Immunol 2009;183:3463–71.
[9] Handel TM, Johnson Z, Rodrigues DH, Dos Santos AC, Cirillo R, Muzio V, et al. An engineered monomer of CCL2 has anti-inflammatory properties emphasizing the importance of oligomerization for chemokine activity in vivo. J Leukoc Biol 2008;84:1101–8.
[10] Crown SE, Yu Y, Sweeney MD, Leary JA, Handel TM. Heterodimerization of CCR2 chemokines and regulation by glycosaminoglycan binding. J Biol Chem 2006;281:25438–46.
[11] Mellado M, Rodriguez-Frade JM, Vila-Coro AJ, Fernandez S, Martin de Ana A, Jones DR, et al. Chemokine receptor homo- or heterodimerization activates distinct signaling pathways. EMBO J 2001;20:2497–507.
[12] Kalinowska A, Losy J. Investigational C-C chemokine receptor 2 antagonists for the treatment of autoimmune diseases. Expert Opin Investig Drugs 2008; 17:1267–79.
[13] Piccinini AM, Knebl K, Rek A, Wildner G, Diedrichs-Mohring M, Kungl AJ. Rationally evolving MCP-1/CCL2 into a decoy protein with potent anti-inflammatory activity in vivo. J Biol Chem 2010;285:8782–92.
[14] McQuibban GA, Gong JH, Tam EM, McCulloch CA, Clark-Lewis I, Overall CM. Inflammation dampened by gelatinase A cleavage of monocyte chemoattractant protein-3. Science 2000;289:1202–6.
[15] McQuibban GA, Gong JH, Wong JP, Wallace JL, Clark-Lewis I, Overall CM. Matrix metalloproteinase processing of monocyte chemoattractant proteins generates CC chemokine receptor antagonists with anti-inflammatory properties in vivo. Blood 2002;100:1160–7.
[16] Proost P, Struyf S, Couvreur M, Lenaerts JP, Conings R, Menten P, et al. Posttranslational modifications affect the activity of the human monocyte chemotactic proteins MCP-1 and MCP-2: identification of MCP-2(6-76) as a natural chemokine inhibitor. J Immunol 1998;160:4034–41.
[17] Rafei M, Hsieh J, Fortier S, Li M, Yuan S, Birman E, et al. Mesenchymal stromal cell-derived CCL2 suppresses plasma cell immunoglobulin production via STAT3 inactivation and PAX5 induction. Blood 2008;112:4991–8.
[18] Zhang YJ, Rutledge BJ, Rollins BJ. Structure/activity analysis of human monocyte chemoattractant protein-1 (MCP-1) by mutagenesis. Identification of a mutated protein that inhibits MCP-1-mediated monocyte chemotaxis. J Biol Chem 1994;269:15918–24.
[19] Egashira K, Nakano K, Ohtani K, Funakoshi K, Zhao G, Ihara Y, et al. Local delivery of anti-monocyte chemoattractant protein-1 by gene-eluting stents attenuates in-stent stenosis in rabbits and monkeys. Arterioscler Thromb Vasc Biol 2007;27:2563–8.
[20] Goser S, Ottl R, Brodner A, Dengler TJ, Torzewski J, Egashira K, et al. Critical role for monocyte chemoattractant protein-1 and macrophage inflammatory protein-1alpha in induction of experimental autoimmune myocarditis and effective anti-monocyte chemoattractant protein-1 gene therapy. Circulation 2005;112:3400–7.
[21] Hayashidani S, Tsutsui H, Shiomi T, Ikeuchi M, Matsusaka H, Suematsu N, et al. Anti-monocyte chemoattractant protein-1 gene therapy attenuates left ventricular remodeling and failure after experimental myocardial infarction. Circulation 2003;108:2134–40.
[22] Ikeda Y, Yonemitsu Y, Kataoka C, Kitamoto S, Yamaoka T, Nishida K, et al. Anti-monocyte chemoattractant protein-1 gene therapy attenuates pulmonary hypertension in rats. Am J Physiol Heart Circ Physiol 2002;283:H2021–8.
[23] Inoshima I, Kuwano K, Hamada N, Hagimoto N, Yoshimi M, Maeyama T, et al. Anti-monocyte chemoattractant protein-1 gene therapy attenuates pulmonary fibrosis in mice. Am J Physiol Lung Cell Mol Physiol 2004;286:L1038–44.
[24] Kumai Y, Ooboshi H, Takada J, Kamouchi M, Kitazono T, Egashira K, et al. Anti-monocyte chemoattractant protein-1 gene therapy protects against focal brain ischemia in hypertensive rats. J Cereb Blood Flow Metab 2004;24: 1359–68.
[25] Nakano K, Egashira K, Ohtani K, Zhao G, Funakoshi K, Ihara Y, et al. Catheter-based adenovirus-mediated anti-monocyte chemoattractant gene therapy attenuates in-stent neointima formation in cynomolgus monkeys. Atherosclerosis 2007;194:309–16.
[26] Ni W, Egashira K, Kitamoto S, Kataoka C, Koyanagi M, Inoue S, et al. New anti-monocyte chemoattractant protein-1 gene therapy attenuates atherosclerosis in apolipoprotein E-knockout mice. Circulation 2001;103:2096–101.
[27] Shimizu H, Maruyama S, Yuzawa Y, Kato T, Miki Y, Suzuki S, et al. Anti-monocyte chemoattractant protein-1 gene therapy attenuates renal injury induced by protein-overload proteinuria. J Am Soc Nephrol 2003;14:1496–505.
[28] Shimizu S, Nakashima H, Masutani K, Inoue Y, Miyake K, Akahoshi M, et al. Anti-monocyte chemoattractant protein-1 gene therapy attenuates nephritis in MRL/lpr mice. Rheumatology (Oxford) 2004;43:1121–8.
[29] Tsuruta S, Nakamuta M, Enjoji M, Kotoh K, Hiasa K, Egashira K, et al. Anti-monocyte chemoattractant protein-1 gene therapy prevents dimethylnitrosamine-induced hepatic fibrosis in rats. Int J Mol Med 2004;14:837–42.
[30] Usui M, Egashira K, Ohtani K, Kataoka C, Ishibashi M, Hiasa K, et al. Anti-monocyte chemoattractant protein-1 gene therapy inhibits restenotic changes (neointimal hyperplasia) after balloon injury in rats and monkeys. FASEB J 2002;16:1838–40.
[31] Yue Y, Gui J, Xu W, Xiong S. Gene therapy with CCL2 (MCP-1) mutant protects CVB3-induced myocarditis by compromising Th1 polarization. Mol Immunol 2011;48:706–13.
[32] Zhao HF, Ito T, Gibo J, Kawabe K, Oono T, Kaku T, et al. Anti-monocyte chemoattractant protein 1 gene therapy attenuates experimental chronic pancreatitis induced by dibutyltin dichloride in rats. Gut 2005;54:1759–67.
[33] Gharaee-Kermani M, McCullumsmith RE, Charo IF, Kunkel SL, Phan SH. CC-chemokine receptor 2 required for bleomycin-induced pulmonary fibrosis. Cytokine 2003;24:266–76.
[34] Gurujeyalakshmi G, Giri SN. Molecular mechanisms of antifibrotic effect of interferon gamma in bleomycin-mouse model of lung fibrosis: downregulation of TGF-beta and procollagen I and III gene expression. Exp Lung Res 1995;21:791–808.
[35] Okuma T, Terasaki Y, Kaikita K, Kobayashi H, Kuziel WA, Kawasuji M, et al. C–C chemokine receptor 2 (CCR2) deficiency improves bleomycin-induced pulmonary fibrosis by attenuation of both macrophage infiltration and production of macrophage-derived matrix metalloproteinases. J Pathol 2004;204:594–604.
[36] Gong JH, Clark-Lewis I. Antagonists of monocyte chemoattractant protein 1 identified by modification of functionally critical NH_2-terminal residues. J Exp Med 1995;181:631–40.
[37] Jarnagin K, Grunberger D, Mulkins M, Wong B, Hemmerich S, Paavola C, et al. Identification of surface residues of the monocyte chemotactic protein 1 that affect signaling through the receptor CCR2. Biochemistry 1999;38:16167–7.
[38] Moore BB, Kolodsick JE, Thannickal VJ, Cooke K, Moore TA, Hogaboam C, et al. CCR2-mediated recruitment of fibrocytes to the alveolar space after fibrotic injury. Am J Pathol 2005;166:675–84.
[39] Russo RC, Garcia CC, Barcelos LS, Rachid MA, Guabiraba R, Roffe E, et al. Phosphoinositide 3-kinase gamma plays a critical role in bleomycin-induced pulmonary inflammation and fibrosis in mice. J Leukoc Biol 2011;89:269–82.
[40] Ponticos M, Holmes AM, Shi-wen X, Leoni P, Khan K, Rajkumar VS, et al. Pivotal role of connective tissue growth factor in lung fibrosis: MAPK-dependent transcriptional activation of type I collagen. Arthritis Rheum 2009;60:2142–55.
[41] Carulli MT, Ong VH, Ponticos M, Shiwen X, Abraham DJ, Black CM, et al. Chemokine receptor CCR2 expression by systemic sclerosis fibroblasts: evidence for autocrine regulation of myofibroblast differentiation. Arthritis Rheum 2005;52:3772–82.

[42] Lubkowski J, Bujacz G, Boque L, Domaille PJ, Handel TM, Wlodawer A. The structure of MCP-1 in two crystal forms provides a rare example of variable quaternary interactions. Nat Struct Biol 1997;4:64–9.
[43] Paavola CD, Hemmerich S, Grunberger D, Polsky I, Bloom A, Freedman R, et al. Monomeric monocyte chemoattractant protein-1 (MCP-1) binds and activates the MCP-1 receptor CCR2B. J Biol Chem 1998;273:33157–65.
[44] Bitterman PB, Rennard SI, Adelberg S, Crystal RG. Role of fibronectin as a growth factor for fibroblasts. J Cell Biol 1983;97:1925–32.
[45] Murray LA, Argentieri RL, Farrell FX, Bracht M, Sheng H, Whitaker B, et al. Hyper-responsiveness of IPF/UIP fibroblasts: interplay between TGFbeta1, IL-13 and CCL2. Int J Biochem Cell Biol 2008;40:2174–82.
[46] Distler JH, Akhmetshina A, Schett G, Distler O. Monocyte chemoattractant proteins in the pathogenesis of systemic sclerosis. Rheumatology (Oxford) 2009;48:98–103.
[47] Baumert J, Schmidt KH, Eitner A, Straube E, Rodel J. Host cell cytokines induced by *Chlamydia pneumoniae* decrease the expression of interstitial collagens and fibronectin in fibroblasts. Infect Immun 2009;77:867–76.
[48] Ghosh AK, Bhattacharyya S, Mori Y, Varga J. Inhibition of collagen gene expression by interferon-gamma: novel role of the CCAAT/enhancer binding protein beta (C/EBPbeta). J Cell Physiol 2006;207:251–60.
[49] Hu B, Wu Z, Jin H, Hashimoto N, Liu T, Phan SH. CCAAT/enhancer-binding protein beta isoforms and the regulation of alpha-smooth muscle actin gene expression by IL-1 beta. J Immunol 2004;173:4661–8.
[50] Marra F, Romanelli RG, Giannini C, Failli P, Pastacaldi S, Arrighi MC, et al. Monocyte chemotactic protein-1 as a chemoattractant for human hepatic stellate cells. Hepatology 1999;29:140–8.
[51] Schecter AD, Berman AB, Yi L, Ma H, Daly CM, Soejima K, et al. MCP-1-dependent signaling in CCR2(−/−) aortic smooth muscle cells. J Leukoc Biol 2004;75:1079–85.